Annu. Rev. Biochem. 1997. 66:233–67

MOLYBDENUM-COFACTOR–CONTAINING ENZYMES: Structure and Mechanism

Caroline Kisker, Hermann Schindelin, and Douglas C. Rees
Division of Chemistry and Chemical Engineering, 147-75CH, California Institute of Technology, Pasadena, California 91125

KEY WORDS: molybdopterin, molybdoenzymes, tungstoenzymes, oxotransferases, molybdenum hydroxylases

ABSTRACT

Molybdenum-containing enzymes catalyze basic metabolic reactions in the nitrogen, sulfur, and carbon cycles. With the exception of the nitrogenase cofactor, molybdenum is incorporated into proteins as the molybdenum cofactor that contains a mononuclear molybdenum atom coordinated to the sulfur atoms of a pterin derivative named molybdopterin. Certain microorganisms can also utilize tungsten in a similar fashion. Molybdenum-cofactor–containing enzymes catalyze the transfer of an oxygen atom, ultimately derived from or incorporated into water, to or from a substrate in a two-electron redox reaction. On the basis of sequence alignments and spectroscopic properties, four families of molybdenum-cofactor–containing enzymes have been identified. The available crystallographic structures for members of these families are discussed within the framework of the active site structure and catalytic mechanisms of molybdenum-cofactor–containing enzymes. Although the function of the molybdopterin ligand has not yet been conclusively established, interactions of this ligand with the coordinated metal are sensitive to the oxidation state, indicating that the molybdopterin may be directly involved in the enzymatic mechanism.

CONTENTS

0066-4154/97/0701-0233$08.00

INTRODUCTION

Molybdenum and tungsten are the only second and third row transition metals that are required for the growth of at least some organisms; molybdenum in particular is an essential trace element for most living systems, including microorganisms, plants, and animals (1). These metals are found associated with a diverse range of redox active enzymes that catalyze basic reactions in the metabolism of nitrogen, sulfur, and carbon (see Table 1). With the exception of nitrogenases that contain an iron-molybdenum-sulfur cluster, molybdenum and tungsten are incorporated into proteins as the molybdenum-cofactor (Mo-co), which contains a mononuclear Mo (or W) atom coordinated to an organic cofactor named molybdopterin. Mo-co–containing enzymes catalyze the transfer of an oxygen atom, ultimately derived from or incorporated into water, to or from a substrate in a two-electron redox reaction. Although most of the detailed characterization of Mo-co type enzymes has, not surprisingly, been achieved with molybdenum-containing proteins, an important recent development is the recognition that certain microorganisms can utilize tungsten in a similar fashion. For historical reasons, there are inconsistencies in the terminology used to designate the molybdenum and tungsten forms of the cofactor; the term Mo-co is used in this article to refer to both forms.

The first structure of an enzyme containing a Mo-co type cofactor to be determined crystallographically was the tungsten-containing enzyme aldehyde ferredoxin oxidoreductase (AOR) from *Pyrococcus furiosus* (2). Subsequently, the structures of two enzymes with the molybdenum-containing form of Mo-co were solved, aldehyde oxidoreductase (or Mop for molybdenum protein) from *Desulfovibrio gigas* (3) and dimethylsulfoxide (DMSO) reductase from *Rhodobacter sphaeroides* (4), followed by the structures of the homologous protein from *Rhodobacter capsulatus* (5, 6). Rather than providing a comprehensive

Table 1 Selected representatives of Mo-co–containing enzyme families[a]

Enzyme	Organism	Subunit composition
DMSO reductase family		
DMSO reductase	*Rhodobacter sphaeroides*	α
	Rhodobacter capsulatus	α
	Escherichia coli	$\alpha\beta\gamma$
Trimethylamine-N-oxide reductase	*Escherichia coli*	α
	Rhodobacter sphaeroides	α
Biotin sulfoxide reductase	*Escherichia coli*	α
Nitrate reductase (dissimilatory)	*Escherichia coli (narGHI)*	$\alpha\beta\gamma$
	Escherichia coli (narZYW)	$\alpha\beta\gamma$
	Paracoccus denitrificans (*napABCD*)	$\alpha\beta\gamma\delta$
Formate dehydrogenase	*Escherichia coli (fdnGHI)*	$\alpha\beta\gamma$
	Escherichia coli (fdoGHI)	$\alpha\beta\gamma$
	Wolinella succinogenes	$\alpha\beta\gamma$
Formate dehydrogenase (W containing)	*Clostridium thermoaceticum*	$\alpha_2\beta_2$
N-formylmethanofuran dehydrogenase (W containing)	*Methanobacterium wolfei*	$\alpha\beta\gamma$
Xanthine oxidase family		
Xanthine oxidase/dehydrogenase	*Bos taurus*	α_2
	Homo sapiens	α_2
	Gallus gallus	α_2
Aldehyde oxidase	*Homo sapiens*	α_2
	Oryctolagus cuniculus	α_2
Aldehyde oxidoreductase	*Desulfovibrio gigas*	α_2
Sulfite oxidase family		
Sulfite oxidase	*Homo sapiens*	α_2
	Rattus norvegicus	α_2
	Gallus gallus	α_2
	Thiobacillus novellis	α
Nitrate reductase (assimilatory)	*Neurospora crassa*	α_2
	Chlorella vulgaris	α_4
	Spinacea oleracea	α_2
Aldehyde ferredoxin oxidoreductase family		
Aldehyde ferredoxin oxidoreductase	*Pyrococcus furiosus*	α_2
Formaldehyde ferredoxin oxidoreductase	*Pyrococcus furiosus*	α_4
Glyceraldehyde-3-phosphate ferredoxin oxidoreductase	*Pyrococcus furiosus*	α
Carboxylic acid reductase	*Clostridium formicoaceticum*	α_4
Aldehyde dehydrogenase	*Desulfovibrio gigas*	α_4
Hydroxycarboxylate viologen oxidoreductase	*Proteus vulgaris*	α_8

[a]Adapted from (15, 17).

survey of Mo-co enzymes, this review focuses on the available structures of Mo-co–containing enzymes, with particular emphasis on the details of the active site geometry and implications of the structural work for the catalytic mechanisms. More detailed discussions of the biochemistry, spectroscopy, and mechanisms of Mo-co enzymes can be found in excellent recent reviews (7–17).

Reactions Catalyzed by Molybdenum-Cofactor–Containing Enzymes

Mo-co–containing enzymes may be generally divided into two categories (14, 15) that are characterized by the types of reactions being catalyzed. The first class contains enzymes such as DMSO reductase and sulfite oxidase that catalyze oxygen atom transfer to or from an available electron lone pair of a substrate. Sequence comparisons and spectroscopic observations (4, 15) show that these enzymes are representatives of two distinct families of Mo-co enzymes, and they are discussed separately in this review. The second category of enzymes is exemplified by xanthine oxidase, *D. gigas* aldehyde oxidoreductase, and *P. furiosus* aldehyde ferredoxin oxidoreductase, which catalyze oxidative hydroxylation reactions of aldehydes and aromatic heterocyclic compounds. The reactions catalyzed by these enzymes are summarized below:

DMSO reductase	$(CH_3)_2S{=}O + 2H^+ + 2e^- \leftrightarrow (CH_3)_2S + H_2O$
Sulfite oxidase	$SO_3^{2-} + H_2O \leftrightarrow SO_4^{2-} + 2H^+ + 2e^-$
Aldehyde oxidoreductase	$R\text{-}CHO + H_2O \leftrightarrow R\text{-}COOH + 2H^+ + 2e^-.$

As indicated in Table 1, these two general reaction categories are presently distributed into four classes of Mo-co–containing enzymes that are described below in more detail.

Common to all these reactions is the cycling between the oxidized Mo(VI) and the reduced Mo(IV) states (or the corresponding oxidation states of W) of the enzyme. It is convenient to consider the overall reaction mechanism as consisting of a coupled pair of reductive and oxidative half-reactions, characterized by the reduction of Mo(VI) and the oxidation of Mo(IV), respectively. Because these enzymes catalyze a two-electron redox reaction to or from the substrate, it is likely that the Mo also directly undergoes a two-electron change in oxidation state during the appropriate half-reaction. The return to the resting state of the enzyme must involve either addition or removal of electrons at the Mo, by means of electron transfer between the Mo and a second redox center. Because the second center is typically a one-electron redox group, such as a heme or iron-sulfur cluster, the Mo is restored to the resting state through a sequence of one-electron transfers that will first generate the intermediate Mo(V) state. As an example, the resting state of DMSO reductase is the Mo(IV) state that binds DMSO, followed by reduction of the substrate to produce dimethylsulfide

(DMS) and the Mo(VI) state of the enzyme. Two subsequent one-electron transfer reactions regenerate the Mo(IV) state after passing through the Mo(V) state. In most cases, the second redox center involved in these electron transfer reactions is contained within the same enzyme molecule as the Mo-co. One notable exception to this general observation is *Rhodobacter* DMSO reductase, which contains no cofactor other than Mo-co. This feature has made this enzyme a valuable target for optical spectroscopy studies (18–21) because the spectral features of the Mo-co are dominated by the much larger absorption of the other prosthetic groups, e.g. iron-sulfur clusters, hemes, and flavins.

Structure and Properties of the Pterin Cofactor in Molybdenum-Cofactor–Containing Enzymes

The discovery of mutations in *Aspergillus niger* resulting in deficient forms of both nitrate reductase and xanthine dehydrogenase led to the suggestion of a common cofactor in these two enzymes, the synthesis of which was assumed to be impaired in these mutations (22). Subsequent studies focused on the delineation of biosynthetic pathways that yield the pterin cofactor, as well as the elucidation of its chemical structure (8, 10). Although controversy remains about some of the biosynthetic steps in the synthesis of the cofactor (23–25), the chemical nature of the cofactor was determined by Rajagopalan and coworkers (8). They postulated a structure for the cofactor (Figure 1*a*) consisting of a pterin derivative, termed molybdopterin, with the pterin ring substituted at position 6 with a phosphorylated dihydroxybutyl sidechain containing a *cis*-dithiolene bond. The sulfur atoms of the dithiolene group were proposed to coordinate the Mo, with a stoichiometry of one molybdopterin per Mo. In bacteria, additional variability of the Mo-co is achieved by attachment of a second nucleotide—GMP (Figure 1), AMP, IMP, or CMP—to the phosphate group of the molybdopterin (10).

The crystal structure of *P. furiosus* AOR (2) established the general validity of this model, with the additional feature that the dihydroxybutyl sidechain actually forms a pyran ring by attack of the 3′-hydroxyl group on C7 of the pterin (Figure 1*b*). Subsequently, this tricyclic form of the pterin was also observed in the crystal structures of *D. gigas* aldehyde oxidoreductase (3) and *R. sphaeroides* (4) and *R. capsulatus* (5, 6) DMSO reductases. The chiral centers at positions 3′, 6, and 7 of the tricycle are in the R-configuration. Ring closure of the pterin may occur upon incorporation of the cofactor into the apo-enzyme and is presumed to be stabilized in the environment provided by the enzyme. As proposed by Rajagopalan (8), the sulfur atoms of the dithiolene group were found to coordinate the metal, either tungsten in *P. furiosus* aldehyde oxidoreductase or molybdenum in *D. gigas* aldehyde oxidoreductase and *Rhodobacter* DMSO reductase, in contrast to some model compounds that showed the pterin ring could also directly coordinate metals (26).

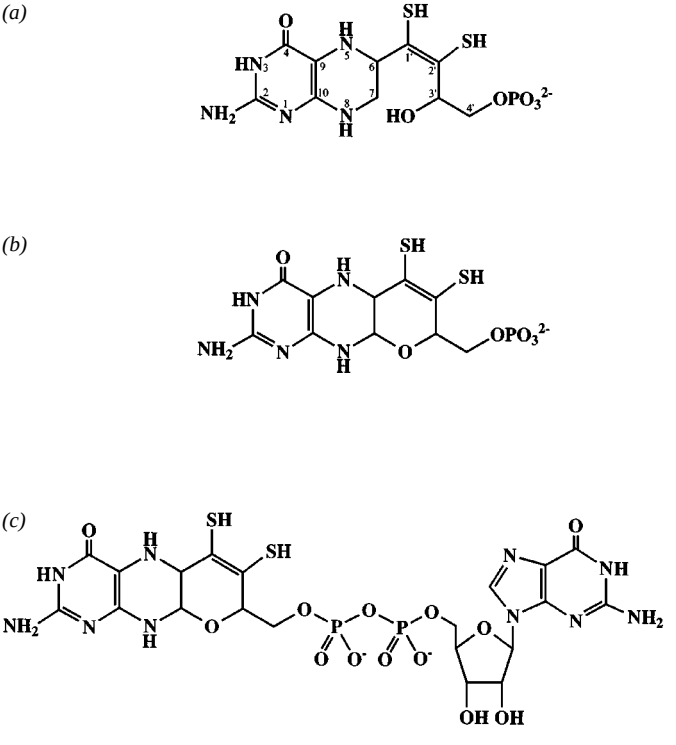

Figure 1 Structure of the pterin cofactor. (*a*) Proposed structure of the pterin cofactor according to Rajagopalan and coworkers (8). The atom numbering scheme of the cofactor is included. (*b*) Structure of the cofactor as first observed in *P. furiosus* aldehyde oxidoreductase. (*c*) Structure of the pterin guanosine dinucleotide cofactor as present in *R. sphaeroides* DMSO reductase.

As demonstrated by the AOR, Mop, and DMSO reductase structures, the tricyclic molybdopterin system is distinctly nonplanar (Figure 2). In particular, the pyran rings adopt a half-chair conformation in these structures that deviates significantly from the plane of the pterin system. In the enzyme bound molybdopterins studied so far, the best plane defined by the pyran ring is tilted $\sim 40^{\circ}$ from the plane of the pterin ring. However, this relationship between rings is not fixed, as a least squares superposition of the pterins in AOR and DMSO reductase reveals conformational flexibility in the way the pyran ring is tilted out of the plane of the conjugated part of the pterin (Figure 2).

As implied by the stereochemistry at positions 6 and 7, the molybdopterin is likely to be in the fully reduced tetrahydropterin oxidation state. Additional support for this conclusion arises from the observation that both N5 and N8 are

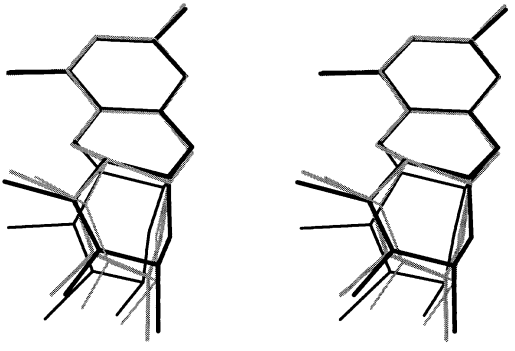

Figure 2 Conformations of the pterin cofactor. Superpositions of the conjugated parts of the pterin cofactors from *R. sphaeroides* DMSO reductase (*thick* and *thin black lines*) and *P. furiosus* AOR (*thick* and *thin grey lines*).

likely to be protonated, because they are used as hydrogen bond donors in the crystal structures analysed so far (Table 2). This behavior argues against the existence of dihydropterin states such as 5,6-dihydropterin and 7,8-dihydropterin, as well as the various quininoid forms of the dihydropterin, because they are not compatible with the observed pattern of hydrogen bond donors and acceptors observed in the known crystal structures. The tetrahydropterin state for the tricyclic structure would likely be equivalent to a dihydropterin (possibly the 5,6-dihydropterin or the 5,8-dihydropterin) in the ring-opened form of the bicyclic pterin.

An unanticipated feature of the *P. furiosus* AOR structure was the observation that the tungsten atom was coordinated not, as anticipated, by one but by two molybdopterins. This situation is not unique to tungstoenzymes, as bismolybdopterin metal coordination was also observed for the molybdenum-containing DMSO reductase. Although the covalent structure of the pterin ring system is identical in all structures, conformational differences are observed, as described above, both between pterins in different proteins and between pterins in the same protein. The two pterins of DMSO reductase differ significantly from each other, whereas the pterins of AOR have an intermediate conformation somewhat more similar to one of the pterins in DMSO reductase. There are also differences in the conformation of the sidechain extending from the tricyclic system. In AOR, this sidechain adopts a conformation such that the phosphate groups of the two molybdopterins are bridged by a single Mg^{2+}. In DMSO reductase and Mop, however, a more extended conformation is observed for the sidechain; for the molybdopterin guanosine dinucleotide (MGD) found in DMSO reductase, the nucleotide and pterin rings are nearly coplanar, whereas

Table 2 Distribution of hydrogen bond donors and acceptors in the pterin ring system of the cofactors in *R. sphaeroides* DMSO reductase (4), *D. gigas* Mop (3), and *P. furiosus* AOR (2)[a]

Atom	DMSO reductase		Mop	AOR	
	P-pterin	Q-pterin		Pterin 1	Pterin 2
N-1	A (either from N737 Nδ2 or from Q440 Nε2)	—	A (from Q807 Nε2)	A (from L495 N)	A (from T344N)
N-2	D (to N737 Oδ1) D (to G754 O)	D (to P644 O)	D (to Q99 Oε1) D (to C139 Sγ)	D (to D489 Oδ1) D (to L493 O)	D (to D338 Oδ1) D (to L342 O)
N-3	D (to A 641 O)	D (either to P644 O or to R647 O)	—	D (to D489 Oδ1)	D (to D338 Oδ1)
O-4	A (from R326 Nη1) ? (H643 Nε2)	A (from H649 N)	A (from T420 N) A (from F421 N)	A (from K 450 Nζ)	—
N-5	D (to E715 Oε1) ? (H643 Nε2)	? (H643 Nδ1)	—	—	—
N-8	D (to H438 O)	D (to T191 O)	D (to Q807 Oε1) A (from Q807 Nε2)	D (C494 Sγ) A (R76 Nη2)	D (D343 Oδ1)

[a]Abbreviations: A, hydrogen bond acceptor; D, hydrogen bond donor; —, denotes atoms not involved in any hydrogen bonded interaction; ?, denotes atoms that could be either the donor or the acceptor in the hydrogen bond. Atom numbers for the pterin are as defined in Figure 1*a*. Atom numbers 2 and 4 specify the exocyclic amino and oxo groups, respectively. Contacts in AOR are only given if they occur in both monomers of the dimer. Only hydrogen bonds with protein atoms are considered.

in the molybdopterin cytosine dinucleotide (MCD) of *D. gigas* aldehyde oxidoreductase, the two nucleotides enclose an angle of about 60° (3).

Enzyme Families Containing the Molybdenum-Cofactor

Until recently, the Mo-co–containing enzymes were divided into two families (14): the xanthine oxidase family containing an oxothio Mo-center, and the sulfite oxidase family, including DMSO reductase and related enzymes supposedly containing a dioxo Mo-center. Classification into either of these families was based upon the inhibitory effects of cyanide, which is a potent irreversible inhibitor of xanthine oxidase and related enzymes. For these enzymes, addition of cyanide triggers the release of a nonpterin sulfur-ligand to the Mo in the form of thiocyanate (27, 28). On the basis of sequence similarities and subtle spectroscopic differences between the isolated Mo-co–containing domain of sulfite oxidase and DMSO reductase, however, the latter enzyme is now believed to represent an independent family of Mo-co–containing enzymes (4, 15). Consequently, three classes of molybdenum-containing Mo-co enzymes are now recognized, represented by DMSO reductase, xanthine oxidase, and sulfite oxidase.

As a result of the relatively recent identification of tungsten-containing proteins, the recognized diversity of Mo-co–containing enzymes has increased (17). The largest family of tungsten-containing enzymes so far characterized is the AOR family, named after the best characterized member, aldehyde ferredoxin oxidoreductase. The AOR class is distinct from the three

presently identified families of Mo-co–containing enzymes. A second family of tungstoenzymes designated the F(M)DH family includes formate dehydrogenase (FDH) and formylmethanofuran dehydrogenase (FMDH). Although the F(M)DH family is clearly distinct from the AOR family, sequence similarities have been detected between the F(M)DH family and the DMSO reductase family, indicating that the F(M)DH family may be included within this class of Mo-co–containing enzymes. Recently, a possible third class of tungsten enzymes was identified, with the isolation of acetylene hydratase from the acetylene-utilizing anaerobe *Pelobacter acetylenicus* (29). Unlike any other known tungstoenzymes or molybdoenzymes, this enzyme catalyzes a hydration, not an oxidation-reduction reaction. In the absence of more extensive characterization of acetylene hydratase, however, we do not include this enzyme in our present discussion of Mo-co–containing enzymes.

A more detailed description of the four currently recognized classes of Mo-co–containing enzymes (DMSO reductase, xanthine oxidase, sulfite oxidase, and AOR; see Table 1) follows, with emphasis on recent crystallographic analyses and their mechanistic implications.

DMSO REDUCTASE FAMILY

Members of the DMSO reductase family are exclusively found in eubacteria and include, among other enzymes, the dissimilatory nitrate reductases, formate dehydrogenases, trimethylamine-N-oxide reductases, and biotin sulfoxide reductases (see Table 1). All these enzymes have MGD as the organic component of their Mo-co. In the absence of oxygen and in the presence of their respective substrates, these enzymes serve as terminal reductases to provide a more efficient energy metabolism, compared to the amount of energy available by fermentation. DMSO reductase is found in a variety of bacteria, including *Escherichia coli* (30), *Rhodobacter sphaeroides* (31), and *Rhodobacter capsulatus* (32). The DMSO reductase from *R. sphaeroides* is a water-soluble single-subunit protein with 780 residues (85 kDa) that contains no cofactor other than Mo-co. In contrast, the *E. coli* enzyme is an integral membrane protein consisting of three subunits: (*a*) the Mo-co–containing A-subunit, (*b*) a B-subunit with four 4Fe:4S clusters, and (*c*) a transmembrane C-subunit also responsible for the binding and oxidation of menaquinol. Electrons are transferred from the C-subunit, via the B-subunit, to the Mo-co. As a result of the enzyme action, a transmembrane proton gradient is established, which is used for the generation of ATP (30). The dissimilatory nitrate reductases have the same architecture as *E. coli* DMSO reductase. Additional interest in DMSO reductase arises from the fact that DMS, the volatile reaction product, is the major component of reduced sulfur in the atmosphere and has been implicated in global climate control (33–35). DMS is produced during zooplankton grazing

on phytoplankton (36) and is subsequently released into the atmosphere, although the global contribution of DMSO reductases to this process is relatively minor.

Structure of DMSO Reductase

DMSO reductase from *R. sphaeroides* was the first enzyme of the DMSO reductase family to be characterized by X-ray crystallography, in both its oxidized and reduced forms at resolutions of 2.2 Å and 2.4 Å resolution, respectively (4). Subsequently, the crystal structure of the highly homologous DMSO reductase from *R. capsulatus* (77% sequence identity) was solved by molecular replacement using *R. sphaeroides* DMSO reductase as the search model (5, 6). An important recent development is the structure determination of the homologous selenocysteine-containing enzyme formate dehydrogenase H from *E. coli*, which contains, in addition to Mo-co, a 4Fe:4S cluster (37).

The polypeptide chain of DMSO reductase folds into four domains (designated I, II, III, and IV) that form a slightly elongated molecule (Figure 3) with overall mainchain dimensions of 75 by 55 by 65 $Å^3$. The spatial arrangement of domains I to III creates a large depression on one side of the molecule resembling a funnel, with the active site located at the bottom of the funnel. The NH_2-terminal domain, or domain I, is formed by two three-stranded antiparallel β-sheets and three α-helices. Domain I is the only domain that forms no direct interactions with the cofactor. Domain II has an α/β-fold, containing a mixed six-stranded β-sheet and nine α-helices distributed on either side of the sheet. The third domain is located on the opposite side of the cofactor relative to the second domain and is also of the α/β type, with a strictly parallel five-stranded β-sheet surrounded by 12 α-helices. The fold of domain III is a variant of the classical dinucleotide binding domain, containing five instead of six parallel β-strands (38). The COOH-terminal domain, or domain IV, is located between the second and third domain on the opposite side of the funnel and consists mainly of a six-stranded β-barrel that contains both antiparallel and parallel strands. Domain IV has the same fold as barwin (39), which belongs to a class of plant defense proteins, and endoglucanase V from *Humicola insolens* (40). Structure-based sequence alignments of the DMSO reductase family of Mo-co–containing enzymes demonstrate that conserved regions are mainly located in the core of domains II and III, as well as in the entire domain IV. The sequence similarities indicate that enzymes of the DMSO reductase family share the same basic architecture, including domains II, III, and IV, as has been observed in DMSO reductase and *E. coli* formate dehydrogenase H.

Active Site Structure

The active sites of the DMSO reductases and *E. coli* formate dehydrogenase were found to contain two MGDs, arbitrarily designated as the P-pterin and the

Figure 3 Overall structure of DMSO reductase. (*a*) Schematic stereo drawing into the active site funnel with the NH_2-terminal domain in black, domain II in light grey, domain III in medium grey, and the COOH-terminal domain in dark grey. The NH_2- and COOH-termini, as well as the residues adjacent to the flexible loop, 380 and 394, are labeled. The cofactor and the sidechain of Ser-147 are shown in ball-and-stick representation. (*b*) Different view of the enzyme after a 90° rotation around the vertical axis of (*a*). All figures of molecular structures have been prepared with MOLSCRIPT (74). Protein Data Bank (PDB) coordinate sets 1CXS and 1CXT were used to prepare illustrations of oxidized and reduced DMSO reductase, respectively.

Q-pterin, that coordinate the Mo with an approximate twofold axis of symmetry passing through the Mo. The active site of DMSO reductase is located at the bottom of the large depression in the protein surface described above. The two halves of the cofactor are arranged in an antiparallel fashion and form an elongated structure with a maxium extent of ~35 Å between the N2 atoms of the two guanine moieties. There are numerous interactions between the protein and cofactor, including 45 direct hydrogen bonds (Figure 4), in addition to a few hydrogen bonds to water molecules, which are not located in the vicinity of the Mo atom. Residues interacting with the cofactor are scattered throughout the linear sequence and are located in domains II, III, and IV. Domains II and III interact primarily with each of the guanosines and share structural similarity, despite the lack of any detectable sequence similarity. A stretch of highly conserved residues forming a polypeptide loop in domain IV is crucial for binding of the two pterin moieties of the cofactor. In addition to the residues interacting with the pterins, the DMSO reductase family of Mo-co–containing enzymes is also characterized by a protein ligand to the Mo. This ligand may be either a serine, like Ser-147 in DMSO reductase; a cysteine; or a selenocysteine as in *E. coli* formate dehydrogenase H.

Although the electron density was well defined for almost all parts of the polypeptide chain, residues 381–393 of *R. sphaeroides* DMSO reductase were found to be disordered in the crystal structure. Residual density near the active site was assigned to the sidechain of Trp-388 in two alternate conformations. In one of them, Trp-388 blocks access to the active site by insertion of its sidechain between the aromatic ring systems of Tyr-165 and Trp-196, leading to stacking interactions. In the other conformation, the sidechain is displaced by approximately 7 Å and is arranged perpendicular to that of Trp-196. These observations suggest that Trp-388 might serve as a lid that can shield the active site when necessary.

In the oxidized, Mo(VI) form of DMSO reductase, the four dithiolene sulfur atoms of the two molybdopterins coordinate the Mo atom in an asymmetric fashion. The two sulfur atoms in the P-pterin, and S1′ in the Q-pterin, are 2.4 Å from the metal, whereas S2′ is 3.1 Å away. The sulfur-sulfur distances in the P and Q-pterins are 3.1 Å and 2.3 Å, respectively, which suggests that there

Figure 4 Schematic representation of hydrogen bonded contacts between protein and cofactor in *R. sphaeroides* DMSO reductase. Contacts to water molecules have been omitted for clarity. The residues are grey shaded with respect to their location in domain II (*light grey*), domain III (*medium grey*), and domain IV (*dark grey*). Hydrogen bonds are indicated by dashed lines, whereas the single long Mo-S2′ (Q-pterin) interaction is shown with a dotted line. The same residues are hydrogen bonded to the cofactor in the reduced form. The only exception is Glu-715, which adopts a different sidechain rotamer conformation.

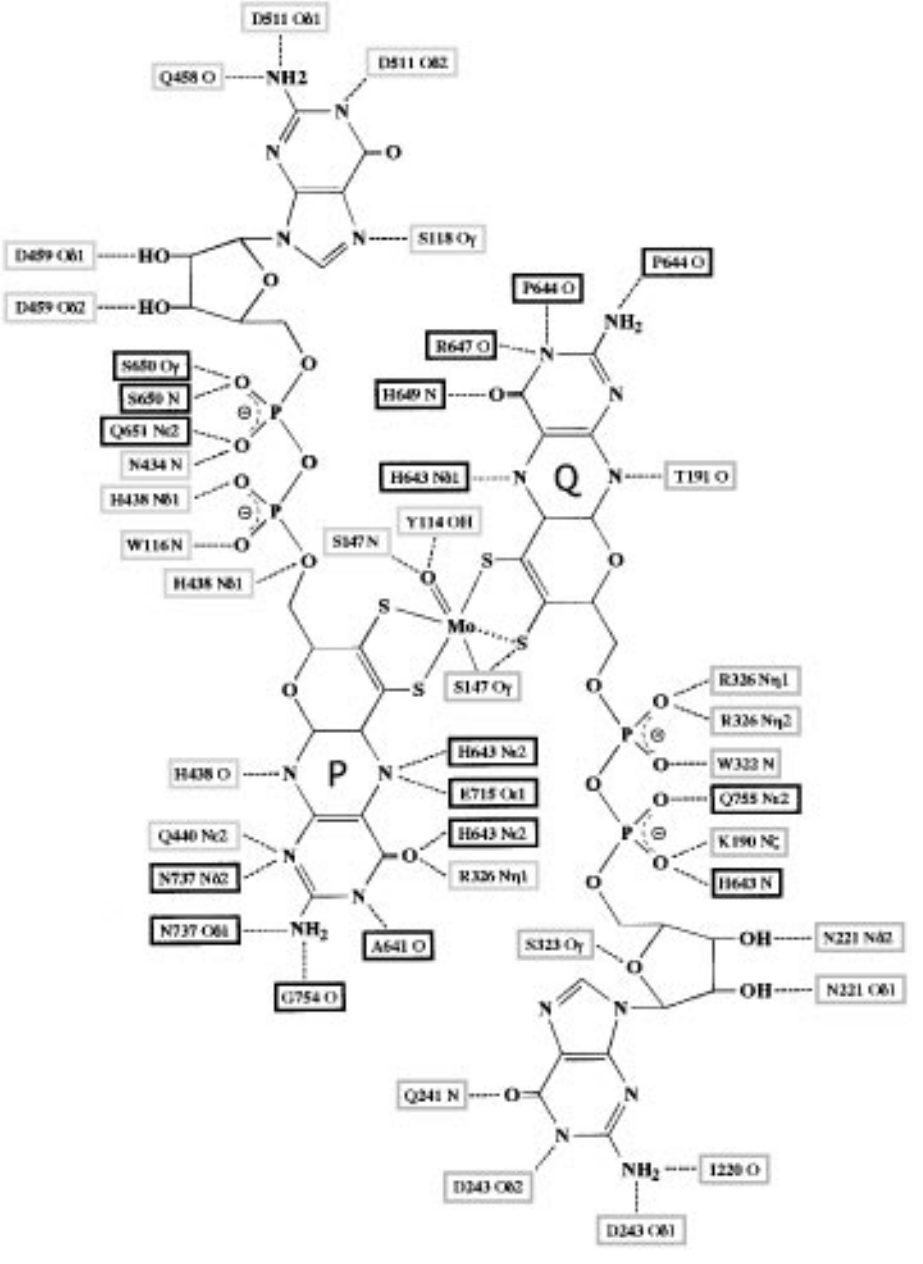

is some disulfide-bond character to the dithiolene group of the Q-pterin. An oxo group, at 1.7 Å distance, forms an additional ligand to the Mo atom, and the coordination sphere is completed by a protein ligand via the sidechain of Ser-147, with a Mo-O distance of 1.7 Å. Thus, the Mo atom is fully coordinated by five ligands and weakly coordinated by a sixth ligand arranged in distorted trigonal bipyramid geometry. The ligands are positioned such that the sulfur atoms of the P-pterin, the Ser-147 Oγ, and the Mo define an equatorial plane, with the oxo group and the S1′ of the Q-pterin positioned as apical ligands on either side of this plane. Consequently, the dithiolene sulfurs of the Q-pterin are positioned approximately *trans* to the oxo group. This positioning suggests that the asymmetric coordination of the Mo by the P and Q-pterins may reflect the influence of the "*trans* effect" (41, 42), in which an oxo group weakens the coordination of a ligand on the opposite side of the metal.

By soaking DMSO reductase crystals in the reductant dithionite, the reduced Mo(IV) form of the enzyme was obtained. Comparison of the two oxidation states did not reveal any major conformational changes in the protein structure. Significant changes were observed at the active site (Figure 5), however, including the expected loss of the oxo-ligand, and a different coordination of the Mo atom by the pterin sulfur atoms. Only three sulfur ligands remained, two in the P-pterin at 2.5 Å from the Mo atom, and one, S1′, in the Q-pterin at 2.9 Å, in addition to Oγ of Ser-147 at 1.8 Å. S2′ in the Q-pterin has shifted to a position 3.7 Å from the Mo atom. Reduction of DMSO reductase is accompanied by an increase in the distance between S1′ and S2′ of the Q-pterin from 2.3 Å to 2.8 Å,

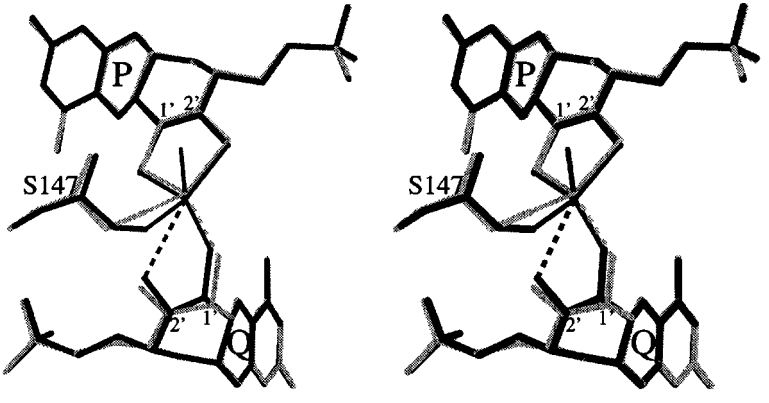

Figure 5 Comparison of the oxidized and reduced forms of DMSO reductase. Superposition of the pterin moieties of the cofactors and Ser-147 in the oxidized (*black*) and reduced form (*grey*). Short coordinating interactions to the Mo are shown with thin solid lines, whereas longer ones are shown with dotted lines.

which suggests that the disulfide-bond character of this interaction is significantly diminished. The sulfur-sulfur distance in the P-pterin, by comparison, remains at 3.1 Å upon reduction. In addition, a keto-enol tautomerization after protonation of the thiolate, and consequent formation of a new chiral center at position 1′ of the Q-pterin have been suggested. Extended X-ray absorption fine structure spectroscopy (EXAFS) studies (43) indicate that the Mo has four sulfur ligands at a distance of 2.44 Å, an oxo group (1.68 Å), and another O/N-ligand (1.92 Å) for the oxidized form of *R. sphaeroides* DMSO reductase. In the reduced form, the number of sulfur ligands was found to decrease to three with an average distance of 2.33 Å; the reduced form also contains an OH-group (1.92 Å) and another O/N-ligand (2.16 Å). Although there are discrepancies between the crystal structure data and the EXAFS data, a decreased number of sulfur ligands in the reduced form is revealed by both techniques. In a crystal structure of the oxidized form of *R. capsulatus* DMSO reductase, a different coordination environment of the Mo has been observed (5). Only two sulfur atoms from the P-pterin, in addition to the Ser sidechain and two oxo groups, were found coordinated to the Mo, in a very similar fashion as in the desulfo form of *D. gigas* aldehyde oxidoreductase (3) (see below). Electron paramagnetic resonance (EPR) spectroscopy has suggested the existence of multiple states of the molybdenum center of *R. capsulatus* DMSO reductase (44). One of the states was found to be similar to the desulfo form of xanthine oxidase, and it seems possible that this is the one that has been observed in this crystal structure. Nevertheless, the reasons for the observed structural differences at the active site are not fully understood.

Mechanism of DMSO Reductase

The reaction catalyzed by DMSO reductase may be subdivided into two half-cycles. In the oxidative half-cycle, the reduced Mo(IV) form of the enzyme binds the substrate, and two electrons are transferred from Mo to the substrate, yielding the reaction product DMS and the oxygen atom of the substrate bound to the metal as an oxo-ligand. In the second, reductive half-cycle, two protons and two electrons are transferred to the metal center, yielding H_2O and regenerating the Mo(IV) state. Since DMSO reductase does not contain a second cofactor that could transfer electrons to Mo-co, an external electron donor, presumably a water-soluble cytochrome, is required for this step.

Based on the observed differences of the coordination of the pterins to the Mo atom in the oxidized and the reduced forms of *R. sphaeroides* DMSO reductase, a reaction mechanism was formulated for the conversion of DMSO to DMS by this enzyme (Figure 6). Direct binding of DMSO to the Mo through either the oxygen atom, or perhaps through both the oxygen and sulfur atoms, should be possible because of the decreased number of metal ligands [three

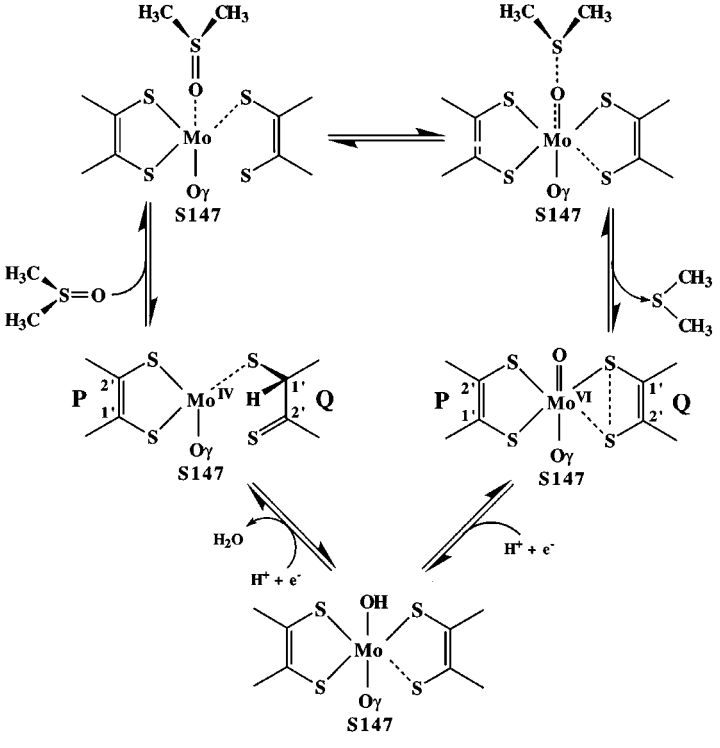

Figure 6 Proposed reaction mechanism of DMSO reductase. Coordination in the Mo(IV) and Mo(VI) states is as observed in the crystal structures of these forms (4). For clarity, the 1′ and 2′ positions in the P- and Q-pterins have been labeled in the Mo(IV) and Mo(VI) states.

pterin sulfurs (with one of them, S1′ of the Q-pterin, at a longer distance) and the sidechain of Ser-147] in the reduced form. Binding of the substrate would lead to a weakening of the sulfur oxygen double bond in the substrate, and liberation of the reaction product DMS could be triggered by a subsequent shift of S1′ and S2′ in the Q-pterin towards the Mo. Concomitantly, Mo would be oxidized to the +VI state, forming a double bond to the oxo-ligand, thus completing the oxidative half-cycle of the reaction with the Mo being coordinated as observed in the oxidized form. According to this mechanism, the oxidation state–dependent interactions of the Q-pterin with the molybdenum would influence the electronic and accessibility properties of the metal, thereby providing some of the necessary requirements for catalysis.

In the reductive half-cycle of the reaction, two cycles of binding of the physiological electron donor to the oxidized enzyme are required. In each cycle

a single electron is transferred to the active site, finally restoring the Mo(IV) state of the enzyme. Two possibilities for the binding of the electron donating cytochrome to DMSO reductase have been suggested. The first possibility is cytochrome binding into the large depression above the active site and possible electron transfer from the cytochrome to the Mo-co mediated by the sidechain of Trp-388 (4). After formation of the Mo(IV) state, a conformational change of Trp-388 could allow entry of DMSO to the active site. The second possibility is cytochrome binding to the surface nearest the pterin moiety of the Q-pterin and electron transfer via the Q-pterin to the Mo (5). This part of the surface is covered by the conserved polypeptide loop in domain IV comprising residues 643–650. These residues mediate many of the protein-cofactor interactions, and the protein surface in this region shows a small depression that is filled with a large number of solvent molecules. This latter mechanism would involve a direct role for a pterin in facilitating electron transfer between the external donor and the oxidized molybdenum center.

According to the proposed mechanism, an oxygen atom is ultimately transferred from the substrate into water, in agreement with ^{18}O labeling experiments (45). This finding is supported by the observed coordination geometry in *R. sphaeroides* DMSO reductase with only one oxo group bound to the Mo, which is the oxygen atom being transferred into water in the reductive half-cycle. One potential candidate for participation in the accompanying proton transfer reaction is the sidechain of Tyr-114, which is hydrogen bonded to the oxo-ligand. The lack of conservation of this residue, however, might indicate that the proton donor can vary among the different members of this family of oxotransferases. Other potential candidates for proton transfer include S2′ of the Q-pterin (via Ser-147, which in turn is well within hydrogen bond distance to the oxo-ligand), water molecules, and other protein sidechains.

XANTHINE OXIDASE FAMILY

Among the members of the xanthine oxidase family (Table 1) are xanthine oxidase, xanthine dehydrogenase, aldehyde oxidase, and the *D. gigas* aldehyde oxidoreductase (3). These enzymes exist as α_2 homodimers and, with the exception of aldehyde oxidoreductase, are all found in eukaryotes. The general architecture of these enzymes comprises four domains starting at the N-terminus with two small domains each containing a single 2Fe:2S cluster, followed by a flavin binding domain (not present in *D. gigas* aldehyde oxidoreductase), and completed by the Mo-co–containing domain (which in the Mop structure was shown to consist of two smaller domains), giving rise to a total molecular weight of approximately 150,000 per monomer. Xanthine oxidase and xanthine dehydrogenase are two different forms of the same enzyme, and

they catalyze the conversion of xanthine to uric acid, a step in the catabolic metabolism of purine bases. The two forms differ in the chemical nature of the oxidizing substrate, O_2 for xanthine oxidase and NAD^+ for xanthine dehydrogenase, and details of the purification procedure determine which form is isolated (46, 47). All enzymes in this family have broad and partially overlapping substrate specificities. EXAFS spectroscopy has shown that the Mo is coordinated by two sulfur ligands originating from the pterin cofactor, the additional cyanide-labile sulfido group, an oxo group, and another oxygen or nitrogen ligand (28, 46). Removal of the cyanide-labile sulfido group results in formation of the inactive desulfo-enzyme, with an oxygen ligand replacing the sulfido group on the Mo.

Structure of Desulfovibrio gigas *Aldehyde Oxidoreductase*

The first structural description of a member of the xanthine oxidase family of Mo-co–containing enzymes was provided for the *D. gigas* aldehyde oxidoreductase, solved at 2.2 Å resolution (3). This protein has been abbreviated as Mop (for molybdenum protein) or AO (for aldehyde oxidoreductase), and the former convention is used in this review. Mop is a dimer composed of two identical 907-residue subunits that each contain a molybdenum coordinated by a single molybdopterin cytosine dinucleotide, and two different 2Fe:2S clusters.

The structure of Mop is organized into four domains that occur sequentially along the polypeptide chain (Figure 7). The first two domains are approximately 75 residues in length and are involved in coordination of the 2Fe:2S clusters. The first cluster-binding domain adopts a fold analogous to that of plant-type 2Fe:2S ferredoxins, whereas the second cluster-binding domain folds into a four-helical bundle that had not been previously observed to coordinate iron-sulfur clusters. The remaining two domains, designated Mo1 and Mo2, are responsible for binding the Mo-co. These domains are substantially larger (386 and 326 residues, respectively) than the two initial domains. A 38-residue-long connecting peptide bridges the 2Fe:2S cluster and the Mo-co binding domains. The Mo1 domain has substantial β-sheet structure with several α-helices, and it provides much of the binding interactions to the molybdopterin. The Mo2 domain contains α/β-structures that form the remaining binding interactions to the molybdopterin, and all of the protein interactions to the cytosine nucleotide. The Mo-co is buried within the Mo1 and Mo2 domains, with active site access provided by a 15 Å–long channel formed at the interface between these two domains. The Mo2 domain also has extensive interactions with the 2Fe:2S cluster–binding domains and has been described as a clamp that holds the domains together.

The structural organization observed in Mop will undoubtedly be observed in xanthine oxidases, given the strong similarities in the amino acid sequences.

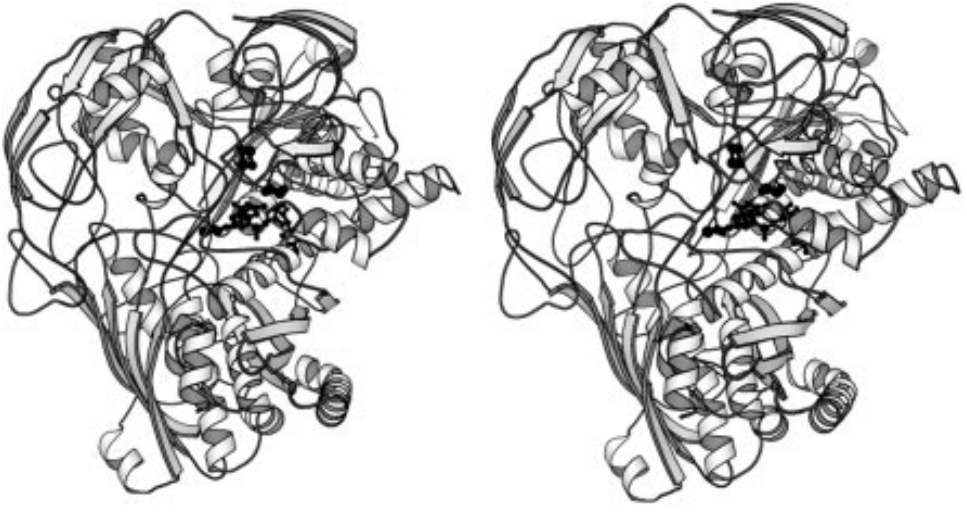

Figure 7 Stereoview of a ribbons representation of the polypeptide fold of the aldehyde oxidoreductase (Mop) from *D. gigas* (3, 48). PDB data set 1ALO was used to prepare this figure.

An important distinction between these two family members, however, is that xanthine oxidase also contains a flavin adenine dinucleotide (FAD) domain. Sequence comparisons indicate that the FAD domain of xanthine oxidase is positioned in the region of the Mop sequence corresponding to the connecting segment. This suggests that the FAD domain will replace the connecting segment found in Mop and may be positioned to contact the 2Fe:2S cluster and the Mo-co binding domains in xanthine oxidase.

Active Site Structure

The initial structure determination of Mop (3) revealed that the Mo was coordinated by the dithiolene sulfurs of a single molybdopterin cytosine dinucleotide, and three nonprotein oxygen ligands. In the absence of a sulfido group to the Mo, this state of Mop likely corresponds to the inactive desulfo form. The pentacoordinate Mo(VI) center exhibits an approximately square pyramidal coordination geometry. The equatorial plane consists of the two dithiolene sulfurs and two oxygen ligands, whereas the remaining ligand, which is sulfido in the active form (48), occupies the apical site (Figure 8*a*). No metal ligands are provided by the protein, although the sidechain of Glu-869, which forms a hydrogen bond to one of the oxygen ligands of the Mo, is sufficiently close (3.5 Å) that a slight rotation could allow binding.

(a)

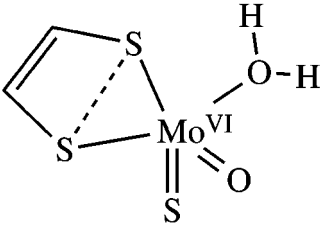

(b)

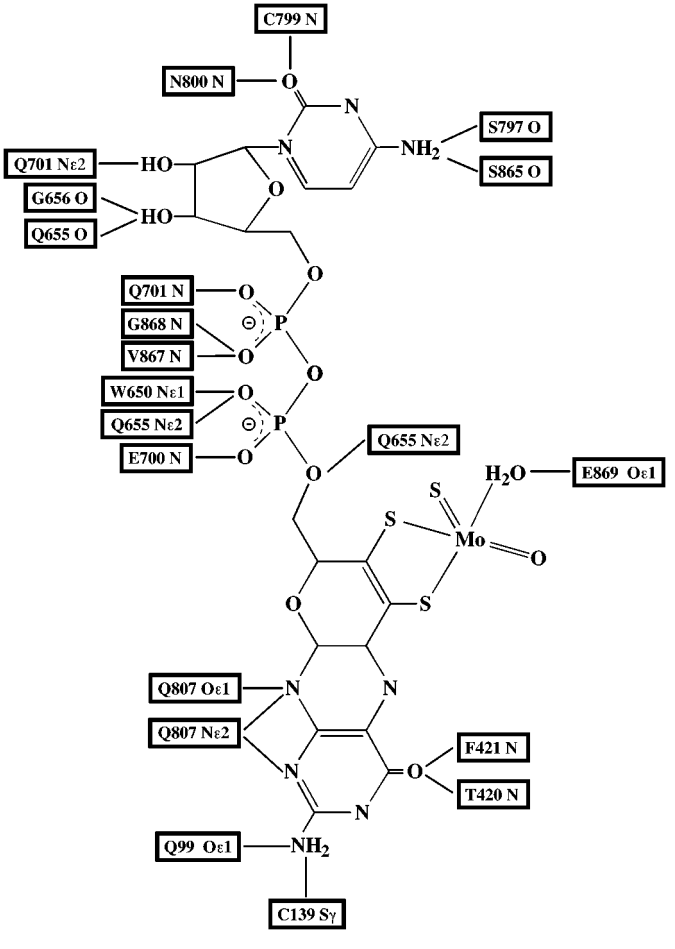

Figure 8 (*a*) Structure of the active site of Mop, with the pterin, oxygen, and sulfido ligands to the Mo indicated (3, 48). (*b*) Schematic representation of hydrogen bonded contacts between protein and molybdopterin in Mop.

The pterin in Mop was found to adopt the tricyclic structure previously established for the pterin cofactor in the *P. furiosus* AOR, thereby demonstrating the basic similarity in the molybdopterin structure between tungsto- and molybdoenzymes. The Mop structure provided the first example of a form of Mo-co that contained a covalently attached nucleotide, in this case a cytosine. The cytosine ring of Mop is extended away from the Mo site, so groups on neither the ribose nor the nucleotide are positioned to coordinate the molybdenum. Both the nucleotide and the molybdopterin rings interact with the protein through multiple hydrogen bonding interactions (Figure 8*b*).

The overall arrangement of metal centers in Mop is such that they are approximately linear, with the Mo and second 2Fe:2S separated by ~15 Å, and the two 2Fe:2S clusters separated by ~12 Å. These distances are somewhat misleading, however, because there are rather direct interactions between metal center ligands. The molybdopterin interacts directly with the second 2Fe:2S cluster of Mop, through a hydrogen bond formed between the N2 atom and the Sγ of the cluster ligand Cys-139. The first and second 2Fe:2S clusters are further linked through a series of covalent and hydrogen bond interactions connecting the two cluster ligands Cys-45 and Cys-137. It seems quite plausible that these interactions facilitate electron transfer from the active site through the 2Fe:2S clusters, with electrons ultimately transferred to an external electron acceptor.

More recently, the identities of the nonprotein metal ligands, including the location of the sulfido group, were established through a series of crystallographic analyses of the desulfo, sulfo, oxidized, reduced, and alcohol-bound forms of Mop at 1.8 Å resolution (48). The sulfido group occupies the apical position of the Mo environment, while the two oxygen ligands in the equatorial site represent water and oxo groups. The sidechain of Glu-869 is hydrogen bonded to the water ligand. Several changes in the environment of the Mo were noticed to occur upon reduction of Mop. The molybdenum shifts toward the apical ligand by 0.4–0.7 Å for the more reduced forms. In addition, the spacing between the dithiolene sulfurs increases from 3.0 Å in the oxidized form to 3.5 Å upon reduction, accompanied by an increased puckering of the ring formed by the dithiolene and molybdenum groups. As in DMSO reductase (4, 5), changes in molybdenum coordination by the pterin ligand occur with alterations in oxidation state of the enzyme. Additionally, it appears that a shorter hydrogen bond from the Glu-869 sidechain oxygen to the bound water occurs upon reduction of Mop.

Mechanistic Implications

Based on the structural studies, a mechanism has been proposed (3, 48) for the oxidation of aldehyde substrates by Mop (Figure 9). The access of substrates to and exit of products from the active site occur through the ~15 Å long

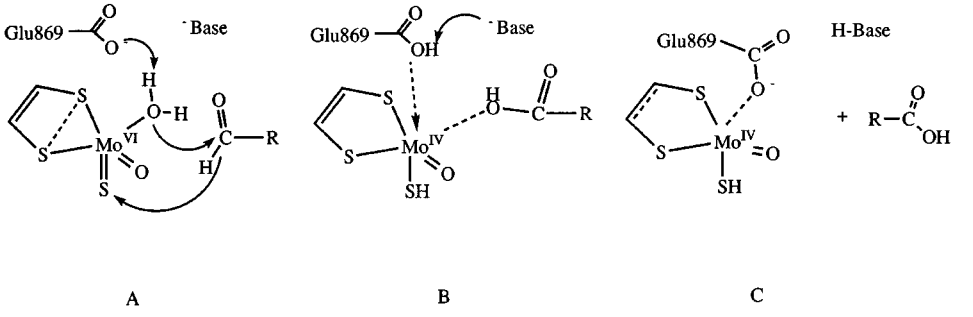

Figure 9 Proposed reaction mechanism of Mop, based on the crystallographic analysis (3, 48). The key events are the nucleophilic attack of the Mo-bound water on the aldehyde carbon, and the hydride transfer from the substrate to the sulfido ligand of the Mo. Partial disulfide bond character in the Mo(VI) state and decreased C=C ditholene double bond character in the Mo(IV) state are indicated.

channel formed between the Mo1 and Mo2 domains that connects the buried molybdenum center to the surface. A likely binding site for substrates in the Michaelis complex, prior to electron transfer, has been identified from the binding site of isopropanol near the equatorial water ligand of the molybdenum. An aldehyde placed at this location would consequently be adjacent to the water ligand and further from the oxo and sulfido ligands. On the basis of this orientation, it is suggested that this water ligand represents the oxygen species that attacks the carbonyl carbon of the substrate, and not an oxo group. The water nucleophile would be transferred as OH^-, after proton transfer to the sidechain of Glu-869. The hydrogen originally bonded to the carbonyl carbon of the substrate is transferred as a hydride to the sulfido group, resulting in reduction of the metal center. Following these events, the product carboxylic acid would be coordinated to the metal [now in the Mo(IV) state] through the transferred oxygen. Product release may be coupled to the binding of the sidechain of Glu-869 to the metal to keep the molybdenum in a pentacoordinate state. After completion of the reductive half-cycle, the Mo(VI) state would be regenerated through a series of one-electron transfers to the 2Fe:2S clusters of Mop by the pathway described above, with the electrons ultimately passed to an external acceptor.

An intriguing aspect of this mechanism is the proposal that a water ligand of the Mo is transferred to the substrate, while a hydride is transferred from the substrate to the enzyme. This mechanism differs from the general mechanism often invoked for Mo-co–containing enzymes, such as DMSO reductase, where an oxo group represents the oxygen species that is transferred between enzyme and substrate. This reasoning is reflected, for example, in the term

oxotransferase that is used to characterize some Mo-co–containing enzymes. For enzymes such as formate dehydrogenases or aldehyde oxidoreductases, however, hydride transfer would also appear to represent a plausible alternative to oxo-group transfer. It is noteworthy, for example, that oxo and hydride transfer occur in the same family of Mo-co enzymes, as exemplified by DMSO reductase and formate dehydrogenase. An important mechanistic objective will be the resolution of the oxo-group versus hydride transfer mechanisms for different Mo-co–containing enzymes.

SULFITE OXIDASE

Sulfite oxidase and the assimilatory nitrate reductases from algae and higher plants form a third group of Mo-co–containing enzymes. These enzymes have a dioxo Mo-center at the active site, with most likely one molybdopterin coordinated to the Mo through the dithiolene sulfur atoms (Figure 10). Members of this family catalyze oxygen atom transfer to or from an electron lone pair of a sulfur or nitrogen atom of the substrate.

Sulfite oxidase is mainly found in eukaryotes and is located in the mitochondrial intermembrane space where it catalyzes the oxidation of sulfite to sulfate. This is the terminal reaction in the oxidative degradation of the sulfur-containing amino acids cysteine and methionine. The enzyme as isolated from different sources has been found to exist as a homodimer of molecular weight 101,000–110,000 that can be proteolytically cleaved into two domains (49). The smaller of these domains, which arises from the N-terminal region of the protein, has a molecular weight of about 10,000 and contains a b_5 cytochrome. The larger C-terminal domain has a molecular weight of about 42,000 and harbors the Mo-co. Both domains are catalytically active following limited proteolysis of the chicken liver enzyme (49, 50).

Assimilatory nitrate reductases catalyze the reduction of nitrate to nitrite, which is then converted to NH_4^+ by nitrite reductase. These nitrate reductases have been found to form homodimers with a molecular weight of ∼220,000 that contain three domains within each subunit. In the case of nitrate reductase from spinach, the N-terminal domain (∼59 kDa) binds the Mo-co, the small central domain (∼14 kDa) contains a *b*-type cytochrome, and the C-terminal domain (∼24 kDa) contains FAD and an $NAD(P)^+$ binding site (51). Sequence comparison between nitrate reductase and sulfite oxidase revealed 31% sequence identity (9) between the N-terminal domain of chicken liver sulfite oxidase (52) and the heme domain of assimilatory nitrate reductase from *Arabidopsis thaliana* (53). The sequence similarities are even more significant in the Mo-co–containing domains, with 38% sequence identity between sulfite oxidase from chicken liver and nitrate reductases from higher plants (9, 52).

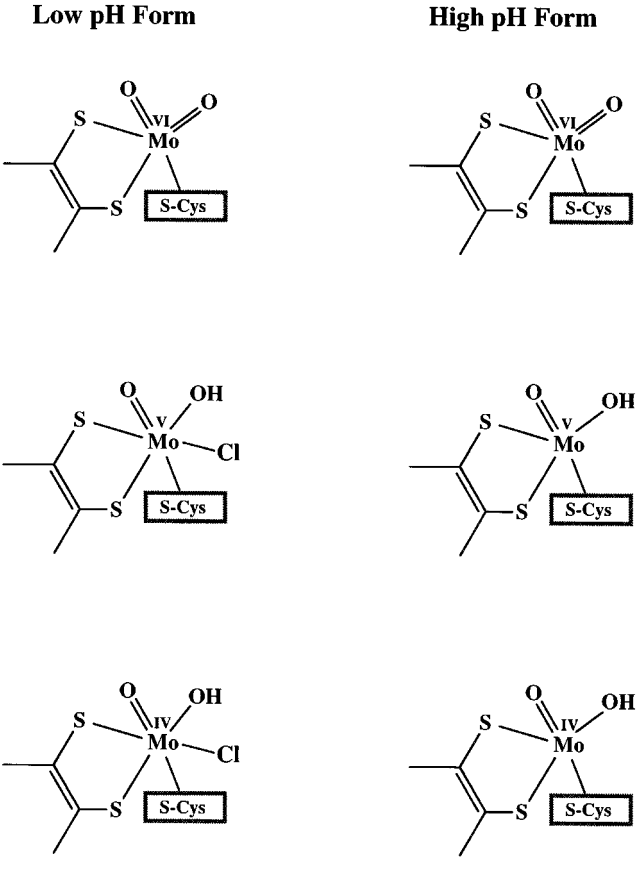

Figure 10 Mo-coordination in sulfite oxidase for the different oxidation states at pH 6.0 and pH 9.0 as determined by EXAFS.

It is possible to clone and express the isolated heme and flavin domains of nitrate reductase (54–56), which seem to fold correctly and maintain many of the properties of the intact enzymes. These results suggest that the domains of both proteins, sulfite oxidase and nitrate reductase, are encoded on contiguous regions in the gene sequence and that these genes once encoded independent proteins that are now fused into one holoenzyme (57). Although the crystal structure of a fragment of corn nitrate reductase comprising the flavin domain has been solved by X-ray crystallography (58), and a model for the cytochrome bound to the flavin domain has been postulated (59), there is at present no three-dimensional structure of the Mo-co domain for this class of enzymes.

Active Site Structure as Defined by EXAFS and EPR Studies

Although no three-dimensional structure is available of the Mo-co domain and the interaction of the Mo and its ligands for any member of the sulfite oxidase family, structural information has been provided by EXAFS and EPR spectroscopies. EXAFS studies (60) with the oxidized enzyme show that two oxygen atoms coordinate the Mo at a distance of 1.71 Å, which according to model compounds should be *cis* to each other (41, 61, 62). In addition to the oxygen atoms, the Mo was also found to be coordinated by three thiolates at a distance of 2.42 Å. This suggests that only one pterin cofactor and not two, as in the DMSO reductase family, coordinate the molybdenum. Two of the three thiolates would be contributed from the pterin cofactor and the third most likely from a cysteine. This residue, Cys-207 in rat and human sulfite oxidase, is conserved in all known sequences of sulfite oxidases and assimilatory nitrate reductases (63). Recent mutagenesis studies of this residue (63) have shown that it is essential for enzyme activity and that it influences the absorption spectrum of the isolated Mo-co–containing domain. Based on the molybdenum coordination environment observed in *D. gigas* aldehyde oxidoreductase (48), it has been postulated (15) that the cofactor dithiolene sidechains, one oxygen ligand, and the Cys-thiolate define the equatorial plane of either a square pyramidal or an octahedral coordination geometry. The second oxo group would occupy one axial position, and the remaining ligand, present only in an octahedral coordination, would occupy the second axial position. The coordination environment of the Mo seems to be very sensitive to the oxidation state of the molybdenum and to the pH of the solution (28, 60). At pH 9.0, all three oxidation states of the molybdenum possess five ligands. At pH 6.0, an additional ligand, most probably chloride, is observed in the Mo(V) and Mo(IV) states. When the enzyme is reduced from the Mo(VI) to the Mo(IV) state, one of the oxygen ligands will be protonated, which is correlated with an increase in bond length from 1.7 Å to ∼2.1 Å (41, 62).

Mechanistic Implications

In the reductive half-cycle of the reaction catalyzed by sulfite oxidase, the Mo is reduced from the (VI) to the (IV) state, coupled to the oxidation of sulfite to sulfate. The reducing equivalents are then singly transferred to the heme center and ultimately passed to cytochrome *c* in the oxidative half-cycle to reestablish the resting Mo(VI) state. Studies of the chemistry of inorganic model compounds (64–70) have helped to improve our understanding of the reaction catalyzed by sulfite oxidase. All model compounds have the composition of L_nMoO_2, in which L is a bulky ligand that prevents the formation of μ-oxo bridged Mo_2 clusters. One of the model compounds is $MoO_2(LNS_2)$ (L = 2,6-bis(2,2-diphenyl-2-mercaptoethyl)pyridine) (64, 65), which is able

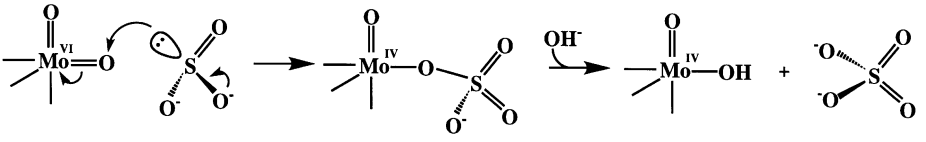

Figure 11 Proposed reaction mechanisms for the conversion of sulfite to sulfate by sulfite oxidase.

to oxidize Ph_3P in the presence of dimethylformamide to yield Ph_3PO. The reduced mono-oxo compound can then be oxidized to its starting complex with dimethylsulfoxide (65). This reaction shows that although the Mo=O bond is known to be stable, an oxygen atom transfer in solution is possible. Another model compound based on a trispyrazolborate ligand (66) reacts in the same way as described above. The significance of this complex is the reaction with water in the presence of an oxidant to obtain the starting compound (68), because this reaction should resemble the mechanism by which the Mo(VI) state of sulfite oxidase is regenerated.

Based on the results from spectroscopic data and studies of model compounds, a catalytic mechanism for sulfite oxidase has been proposed (14) (Figure 11). The initial binding of sulfite at the active site could either be a direct coordination of the substrate to the Mo or more likely, a nucleophilic attack of the lone pair of sulfite, which is a good oxo-group acceptor, on one of the Mo=O bonds. In the latter case, a bidentate intermediate would be observed, which would lead to an intermediate resembling the phosphate-complexed Mo(V) signal as observed in EPR studies of sulfite oxidase (71). In a very recent study (72), the Mo-P distance of either one or two bound phosphates was calculated to be 3.24 Å, with the bound phosphate(s) freely rotating around the Mo-O bond. Subsequently, sulfate would be released by replacement with a hydroxide from the solvent. The catalytic cycle would be completed by two single-electron transfers to the heme of the enzyme and concomittant deprotonation leading to the resting dioxo Mo-center. It seems very likely that only one of the two oxygen ligands is the catalytically labile oxygen, whereas the other oxygen cannot be attacked owing to steric hindrance in the active site of the enzyme.

ALDEHYDE FERREDOXIN OXIDOREDUCTASE FAMILY

As implied by the name, members of the AOR family catalyze the interconversion of aldehydes to carboxylates. Many of the members of the AOR family are tungsten proteins, including formaldehyde ferredoxin oxidoreductase (FOR) and glyceraldehyde-3-phosphate ferredoxin oxidoreductase (GAPOR), that, like AOR, are isolated from hyperthermophilic archeons. In addition, the

AOR family also contains a carboxylic acid reductase that is found in certain acetogenic clostridia, and an aldehyde dehydrogenase from *D. gigas* (an enzyme that is distinct from Mop) (17). Although the functions of these proteins have not all been established, AOR itself likely plays an important role in peptide fermentation, with the substrate aldehydes generated by the transamination and subsequent decarboxylation of amino acids. AOR, FOR, and GAPOR appear specific for tungsten; cell growth under conditions of excess molybdenum and only trace amounts of tungsten results only in production of the tungstoenzymes. A molybdenum-containing member of this family does occur, however; it is the hydroxycarboxylate viologen oxidoreductase from *Proteus vulgaris*, which apparently cannot utilize tungsten (72a). What factors influence the choice of metals used by Mo-co enzymes remains a question of great interest.

Structure of Pyrococcus furiosus *Aldehyde Ferredoxin Oxidoreductase*

AOR from the hyperthermophile *Pyrococcus furiosus* was the first Mo-co–type enzyme to be structurally characterized, thereby establishing the structure of the metal-coordinating pterin illustrated in Figure 1*b*. AOR is a dimer of two identical 605-residue (66 kDa) subunits of known sequence. Three different types of metal sites are found in the AOR protein dimer, including two copies of the tungsten center, two copies of a 4Fe:4S cluster, and a single metal atom located at the dimer interface. The crystallographic structure of AOR (Figure 12) established that a tungsten cofactor and 4Fe:4S cluster are positioned in close proximity within each subunit (the closest distance is $\sim$8 Å between metals). The mononuclear tetrahedral metal center is most likely Fe and is positioned on the dimer two-fold axis $\sim$25 Å from the other metal centers. The 4Fe:4S clusters and tungsten cofactors in different subunits of the dimer are separated by $\sim$50 Å. Each subunit of AOR folds into three domains, with the binding sites for the tungsten cofactor and 4Fe:4S cluster located at the interfaces of these domains. Domain 1 contains a 12-stranded antiparallel β-barrel, whereas the regular secondary structure of domains 2 and 3 consists primarily of α-helices, with little β-structure. The overall polypeptide fold of AOR, as well as individual domains, reveals no obvious structural similarities to the DMSO reductase and Mop folds; indeed the comparison of the AOR structure to structures in the Protein Data Bank indicates that AOR exhibits a unique fold. Domain 1 (residues 1–210) forms a base on which the saddle-like tungsten pterin cofactor sits, whereas domains 2 (residues 211–417) and 3 (residues 418–605) enclose the opposite surface of the tungsten cofactor and provide residues that form specific polar and ionic interactions with the different metal centers. The polypeptide fold of domain 1 exhibits a pseudo twofold axis that coincides approximately with the twofold axis of the tungsten cofactor (see below). A

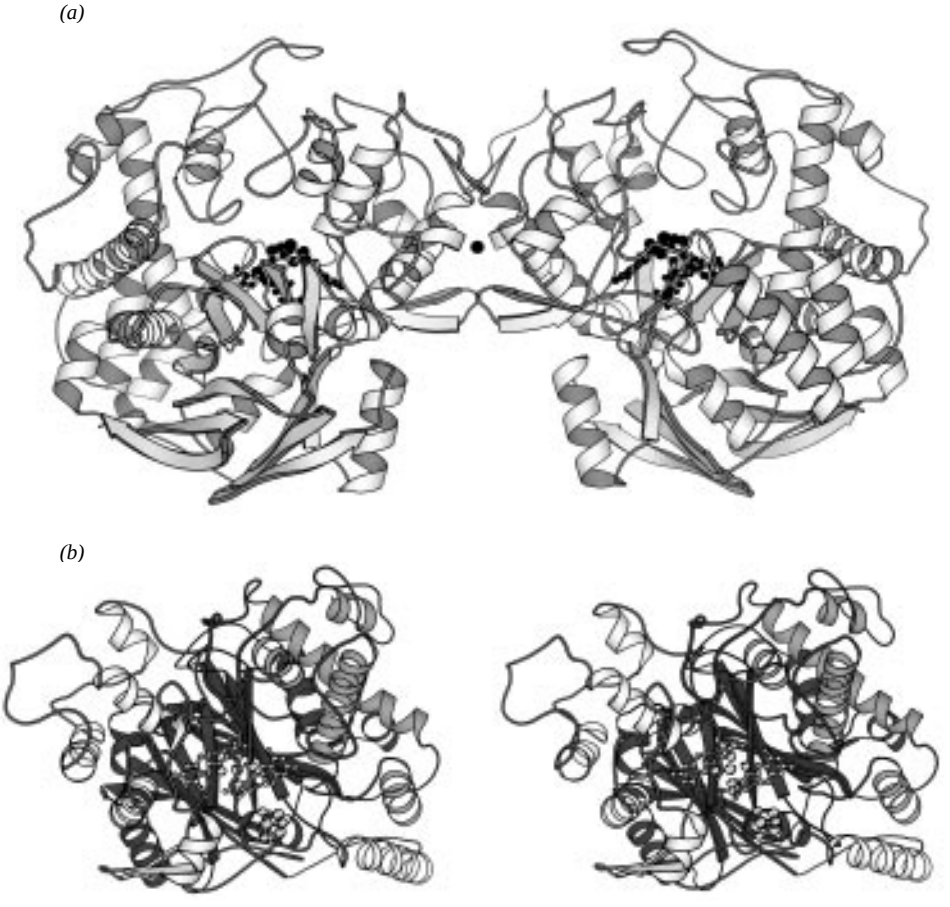

Figure 12 (*a*) Ribbons diagram illustrating the polypeptide fold in the AOR dimer. (*b*) Stereoview of a ribbons diagram of a single subunit of AOR, viewed approximately down the twofold axis of the pterin cofactor. The cofactors are represented by ball-and-stick models. In (b), domains I, II, and III are shaded black, light grey, and medium grey, respectively. PDB data set 1AOR was used to prepare figures of AOR.

channel, formed at the interface between domains 2 and 3, that straddles this twofold axis is likely to provide substrate access to the tungsten center.

Active Site Structure

The tungsten ion in AOR is symmetrically coordinated by the four dithiolene sulfurs from the two molybdopterins bound to each subunit (Figure 13*a*). The presence and location of oxo groups coordinated to the tungsten could not be definitely established crystallographically, perhaps owing to either disorder

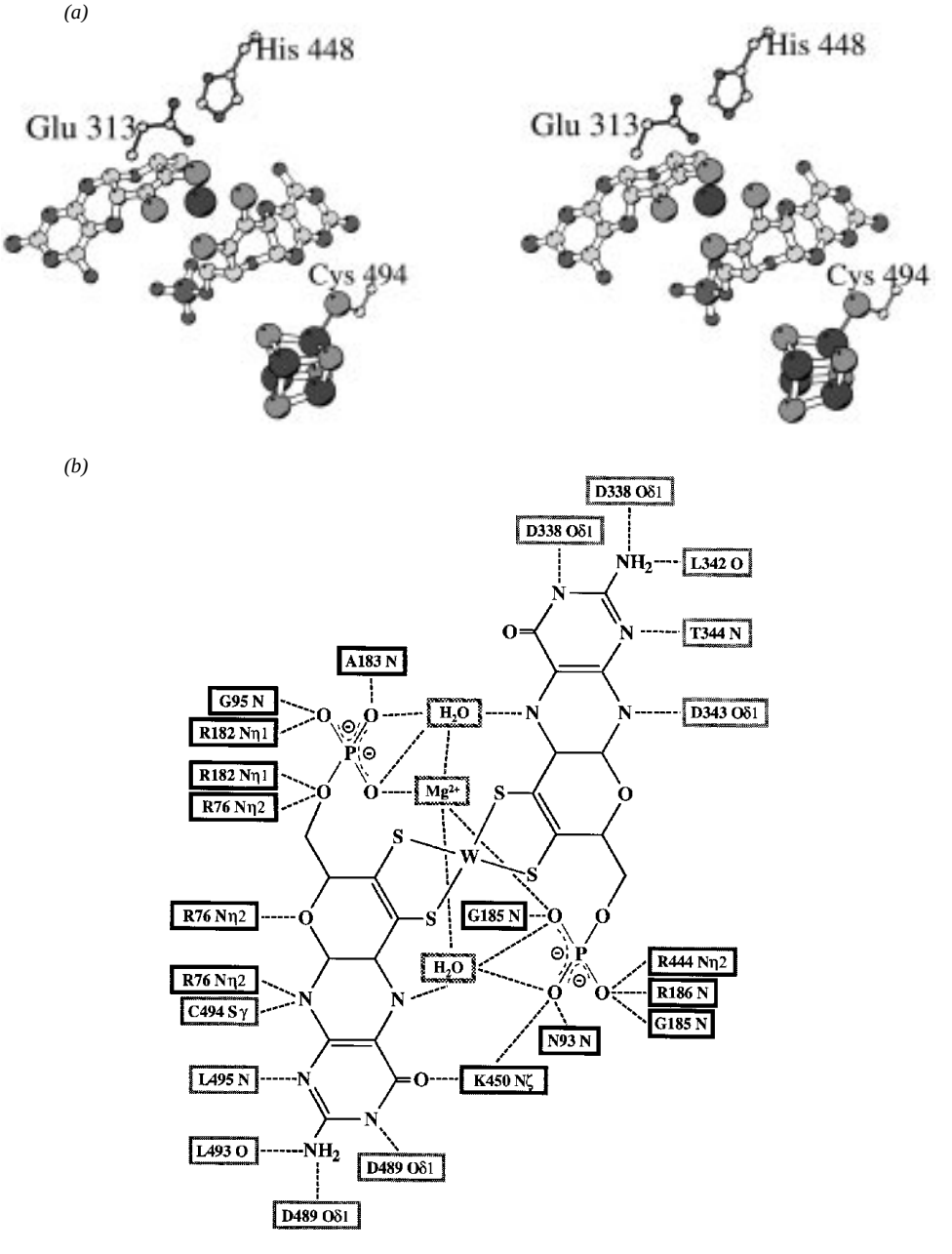

Figure 13 (*a*) Stereoview of the active center of AOR, with the tungsten, the molybdopterin cofactor, the 4Fe:4S cluster, and the neighboring sidechains of Glu-313 and His-448. The phosphate group of the upper molybdopterin has been removed for clarity. (*b*) Schematic representation of hydrogen bonded contacts between protein and molybdopterins in AOR. Residues are shaded according to their location in domains I (*black*), II (*light grey*), and III (*medium grey*), respectively.

at this center or to crystallographic problems associated with locating light atoms in the vicinity of heavy metals. No protein ligands are coordinated to the tungsten, although the sidechains of residues Glu-313 and His-448 are in the vicinity of the tungsten and could participate in proton transfer reactions coupled to electron transfers. The arrangement of the tungsten and the two pairs of dithiolene sulfurs may be described as a distorted square pyramid. The bond distances between the tungsten and sulfurs average 2.34 Å. The base of the pyramid is defined by pairs of sulfurs separated by ~3.0 Å on each edge, both for sulfurs in the same and different dithiolene groups. The tungsten is positioned ~1 Å above the least-squares plane defined by the four sulfurs, which in turn deviate by an average of ~0.3 Å from this plane. The dithiolene groups are tilted by ~80° with respect to each other. The geometry of the WS_4 center is such that if one or more oxo groups are present in the open coordination sites, they would not be *trans* to any of the W-S bonds. This expectation is consistent with the absence of any long W-S bonds, as occurs in model systems when an oxo group is *trans* to a sulfur (41, 42, 73).

In addition to interactions between the dithiolene sulfurs and tungsten, the two molybdopterin ligands are also linked through their phosphate groups, which coordinate axial sites of the same magnesium ion. The two molybdopterin ligands are approximately related by a twofold rotation about an axis that passes through both the tungsten and magnesium sites. The magnesium ion exhibits octahedral geometry, with two coordination sites filled by phosphate oxygens, two sites provided by backbone carbonyl oxygens from residues Asn-93 and Ala-183, and two water molecules. The two waters form part of a hydrogen bonding network within the tungsten cofactor. Each water is hydrogen bonded to at least one phosphate oxygen and an N5 nitrogen of the pterin ring, with one of the two waters also within hydrogen bond distance of the pyran oxygen of one of the molybdopterin ligands. Interactions with the phosphates are provided by the sidechains of Lys and Arg residues, as well as by amide nitrogens of the peptide backbone (Figure 13*b*).

Multiple hydrogen bonding interactions are also formed between the protein and molybdopterin rings (Figure 13*b*). For example, a set of similar interactions with each pterin ring is provided by residues 338–344 and 489–495 in domains 2 and 3, respectively. These stretches contain the sequence Asp-X-X-Gly-Leu-(Cys or Asp)-X, where the carboxylate group of the first Asp and Leu mainchain carbonyl oxygen are arranged to bind the exocyclic N2 group of their respective pterin. Asp-343 and Cys-494 interact with the secondary ring nitrogen, N8, near the pyran ring, whereas the amide nitrogens from the C-terminal end of each motif, Thr-344 and Leu-495, form a hydrogen bond with the secondary ring nitrogen N3 on the pterin. This sequence motif occurs in both domains at the end of α-helices. However, as the Mop and DMSO reductase structures demonstrate, this motif does not represent a universal pterin binding sequence.

The 4Fe:4S cluster is positioned approximately 10 Å from the tungsten atom in AOR and is buried ~6 Å below the van der Waals surface of the protein. This arrangement is consistent with the postulated role of the 4Fe:4S cluster as an intermediary for electron transfer between the tungsten cofactor and ferredoxin, the physiological electron acceptor of AOR. Four thiolate ligands, provided by Cys-288, Cys-291, Cys-295, and Cys-494, coordinate the 4Fe:4S cluster. The 4Fe:4S cluster is linked to one of the two molybdopterins of the tungsten cofactor by two distinct sets of interactions. The sidechain of Arg-76 bridges these two groups by forming hydrogen bonds to an inorganic sulfur of the 4Fe:4S cluster, and to three sites on the molybdopterin ring: N8, the pyran oxygen, and a phosphate oxygen. In addition, the Sγ of Cys-494, a 4Fe:4S cluster ligand, is positioned to accept a hydrogen bond from the pterin ring nitrogen N8. The relationship between the iron sulfur cluster and the molybdopterin in AOR is very different from that observed in Mop, where the 2Fe:2S cluster interacts with the N2 nitrogen. In both cases, however, interactions could provide electron transfer pathways between the metal and the iron-sulfur cluster. This arrangement suggests that the pterin ligand does not merely play a passive structural role but may be an active participant in the redox chemistry of Mo-co–containing enzymes.

A key issue in the structural analysis concerns the detailed coordination environment and oxidation state of the tungsten in both the crystal and solutions of AOR. This analysis is complicated by the heterogeneous nature of the tungsten center in the as-isolated form of AOR in dithionite, with W(IV), W(V), and W(VI) oxidation states all present (17). Spectroscopic and electrochemical characterizations further indicate that several forms of the tungsten center are present in AOR, including both active and inactive forms. The W(V) state of the catalytically active form of AOR likely has the tungsten coordinated to three dithiolene sulfurs, with the fourth sulfur more weakly coordinated, in addition to single oxo and hydroxyl groups. This behavior suggests some similarities to the active site of DMSO reductase, although unlike the situation with DMSO reductase, no crystallographic evidence for asymmetric sulfur coordination of the metal in AOR has yet been observed. In contrast to the catalytically active state of AOR, in at least one inactive form two oxo groups are likely present in the W(VI) state. The inability of the crystallographic analysis to unambiguously identify the presence and number of oxo groups may reflect the presence of multiple forms of AOR in the crystal, including both active and inactive forms.

Mechanistic Implications

Little is known about the mechanistic details of AOR, especially concerning the possibility of oxo-group or hydride-transfer reaction mechanisms. At present, the crystal structure can only provide some general constraints on substrate binding and the reaction mechanism. As with Mop, the active site of AOR is

buried within the protein, with substrate access provided by a channel leading to the protein surface. The dimensions of this channel likely place restrictions on the substrate size such that AOR has a preference for aldehyde derivatives of common amino acids. Unless substantial rearrangements in the tungsten coordination sphere occur during substrate oxidation, the presence of two molybdopterin ligands in AOR enforces *cis* coordination for the substrate and nonpterin groups, which would have stereochemical consequences for the oxygen transfer and oxidation-reduction reaction mechanisms. Further spectroscopic, biochemical, and structural studies are needed to more precisely define the reaction mechanism.

PERSPECTIVE AND OUTLOOK

The recent structure determinations of AOR, Mop, and DMSO reductase have provided the first atomic resolution glimpses of both the active site and the polypeptide fold of Mo-co–containing enzymes. Although this is a small sampling compared to the large number of Mo-co–containing enzymes, these enzymes do represent three of the four currently identified classes. Hence, it is irresistible to draw some generalizations from the available structures:

1. Molybdopterin cofactors are not associated with a unique polypeptide fold. Rather, it is clear that different protein folds can accommodate binding of the cofactors. An important role for the protein appears to provide a predominantly buried environment for the metal site with regulated access for ligand binding. In this regard, pterins are rather like hemes or flavins in that these cofactors are found bound to a diverse set of proteins.

2. In all Mo-co enzymes structurally characterized to date, the molybdopterin adopts a nonplanar tricyclic system with a pyran ring fused to the pterin system. Metal coordination by the pterin occurs through the dithiolene sulfur groups, with the remaining coordination sites occupied by nonprotein ligands such as oxo groups, water, or sulfur-containing groups; in some enzymes such as DMSO reductase and formate dehydrogenase, amino acid sidechains may also bind to the metal. In the well characterized enzymes studied to date, it appears that at least three sulfur ligands to the metal are required for activity.

Not surprisingly, many questions about the Mo-co remain unanswered:

1. What is the mechanism of Mo-co–catalyzed enzymes? Although substantial progress has been made in elucidating reaction mechanisms for some enzymes, such as xanthine oxidases and DMSO reductase, there are still many enzymes for which even basic mechanistic information (such as oxo-group versus hydride transfer) is not available.

2. What factors influence the incorporation of tungsten instead of molybdenum in some enzymes? The answer may reflect bioavailability considerations, but there are also chemical differences between Mo and W, such as the relative difficulty of reducing tungsten to the W(IV) state, and the enhanced bond strength of W(VI) complexes, that might be relevant (17).

3. Will metals other than molybdenum or tungsten be found to be coordinated by the molybdopterin ligand? Vanadium might be one such metal, as it is known to substitute for molybdenum in certain nitrogenases.

4. What is the role of the molybdopterin? Changes in the molybdopterin conformation and interaction with the metal have been observed for DMSO reductase and Mop. It seems likely that pterins can participate in the reaction and electron transfer mechanisms of these enzymes, although this has not been directly demonstrated. The molybdopterin will also help establish the redox potential of the metal center, and variations in the conformations and number of pterins between different proteins may be related to this effect. The functional significance of a nucleotide component of Mo-co, when present, is unclear.

5. How is the Mo-co assembled and inserted into the enzyme? Aspects of the assembly of Mo-co, including the biosynthesis of the molybdopterin, details of metal insertion, and the introduction of the cofactor into the protein (which probably occurs prior to the completion of folding given the size of the cofactor and the almost complete burial of the cofactor within the protein) represent fascinating, and unresolved, problems.

The convergence of biochemical, spectroscopic, chemical, and structural approaches has started to provide a molecular-level understanding of the mechanisms of molybdenum-cofactor–containing enzymes. Although this understanding is still far from complete, we anticipate, based on the rate of recent developments, rapid progress in deciphering the mechanistic details by which these enzymes catalyze some of the key transformations in the nitrogen, sulfur, and carbon cycles of the biosphere.

ACKNOWLEDGMENTS

Supported by Deutsche Forschungsgemeinschaft postdoctoral fellowships (to CK and HS) and by USPHS grant GM50775 (to DCR). The authors would like to thank group members and MWW Adams, J Enemark, J Hilton, MK Johnson, and KV Rajagopalan for stimulating discussions and collaborations on Mo-co–containing enzymes.

Literature Cited

1. Stiefel EI. 1993. See Ref. 11, pp. 1–19
2. Chan MK, Mukund S, Kletzin A, Adams MWW, Rees DC. 1995. *Science* 267:1463–69
3. Romäo MJ, Archer M, Moura I, LeGall J, Engh R, et al. 1995. *Science* 270:1170–76
4. Schindelin H, Kisker C, Hilton J, Rajagopalan KV, Rees DC. 1996. *Science* 272:1615–21
5. Schneider F, Löwe J, Huber R, Schindelin H, Kisker C, Knäblein J. 1996. *J. Mol. Biol.* 263:53–69
6. McAlpine AS, Bailey S. 1996. *Int. Union Crystallogr. Abstr.* C-136
7. Bray RC. 1988. *Q. Rev. Biophys.* 21:299–329
8. Rajagopalan KV. 1991. *Adv. Enzym.* 64:215–90
9. Wootton JC, Nicholson RE, Cock JM, Walters DE, Burke JF, et al. 1991. *Biochim. Biophys. Acta* 1057:157–85
10. Rajagopalan KV, Johnson JL. 1992. *J. Biol. Chem.* 267:10199–202
11. Stiefel EI, Coucouvanis D, Newton NW, eds. 1993. *Molybdenum Cofactors and Model Systems*, Vol. 535. Washington, DC: Am. Chem. Soc. 387 pp.
12. Enemark JH, Young CG. 1993. *Adv. Inorg. Chem.* 40:1–88
13. Pilato RS, Stiefel EI. 1993. In *Bioinorganic Catalysis*, ed. J Reedijk, pp. 131–88. New York: Marcel Dekker
14. Hille R. 1994. *Biochim. Biophys. Acta* 1184:143–69
15. Hille R. 1996. *Chem. Rev.* 96:2757–2816
16. Hille R. 1996. *J. Biol. Inorg. Chem.* 1:397–404
17. Johnson MK, Rees DC, Adams MWW. 1996. *Chem. Rev.* 96:2817–39
18. Bastian NR, Kay CJ, Barber MJ, Rajagopalan KV. 1991. *J. Biol. Chem.* 266:45–51
19. Benson N, Farrar JA, McEwan AG, Thomson AJ. 1992. *FEBS Lett.* 2:169–72
20. Finnegan MG, Hilton J, Rajagopalan KV, Johnson MK. 1993. *Inorg. Chem.* 32:2616–17
21. Kilpatrick L, Rajagopalan KV, Hilton J, Bastion NR, Stiefel EI, et al. 1995. *Biochemistry* 34:3032–39
22. Pateman JA, Cove DJ, Rever BM, Roberts DB. 1964. *Nature* 201:58–60
23. Hinton SM, Dean D. 1990. *Crit. Rev. Microbiol.* 17:169–88
24. Wuebbens MW, Rajagopalan KV. 1995. *J. Biol. Chem.* 270:1082–87
25. Irby RB, Adair WL. 1994. *J. Biol. Chem.* 269:23981–87
26. Fischer B, Schmalle H, Dubler E, Schäfer A, Viscontini A. 1995. *Inorg. Chem.* 34:5726–34
27. Massey V, Edmondson DE. 1970. *J. Biol. Chem.* 245:6595–98
28. Cramer SP, Wahl R, Rajagopalan KV. 1981. *J. Am. Chem. Soc.* 103:7721–27
29. Rosner BM, Schink B. 1995. *J. Bacteriol.* 177:5767–72
30. Weiner JH, Rothery RA, Sambasivarao D, Trieber CA. 1992. *Biochim. Biophys. Acta* 1102:1–18
31. Satoh T, Kurihara FN. 1987. *J. Biochem.* 102:191–97
32. McEwan AG, Ferguson SJ, Jackson JB. 1991. *Biochem. J.* 274:305–7
33. Chanson RJ, Lovelock JE, Andreae MO, Warren SG. 1987. *Nature* 326:655–61
34. Bates TS, Chanson RJ, Gammon RH. 1987. *Nature* 329:319–21
35. Stiefel EI. 1996. *Science* 272:1599–1600
36. Dacey JWH, Wakeham SG. 1986. *Science* 233:1314–16
37. Boyington JC, Gladyshev V, Stadtman TC, Sun PD. 1996. *Int. Union Crystallogr. Abstr.* C-128
38. Schulz GE. 1992. *Curr. Opin. Struct. Biol.* 2:61–67
39. Ludvigsen S, Poulsen FM. 1992. *Biochemistry* 31:8783–89
40. Davies GJ, Dodson GG, Hubbard RE, Tolley SP, Dauter Z, et al. 1993. *Nature* 365:362–64
41. Stiefel EI. 1977. *Prog. Inorg. Chem.* 21:1
42. Holm RH. 1987. *Chem. Rev.* 87:1401–49
43. George GN, Hilton J, Rajagopalan KV. 1996. *J. Am. Chem. Soc.* 118:1113–17
44. Bennett B, Benson N, McEwan AG, Bray RC. 1994. *Eur. J. Biochem.* 225:321–31
45. Schultz BE, Hille R, Holm RH. 1995. *J. Am. Chem. Soc.* 117:827–28
46. Turner NA, Bray RC, Diakun GP. 1989. *Biochem. J.* 260:563–71

47. Battelli MG, Lorenzoni E, Stirpe F. 1973. *Biochem. J.* 131:191–95
48. Huber R, Hof P, Duarte RO, Moura JJG, Moura I, et al. 1996. *Proc. Natl. Acad. Sci. USA* 17:8846–51
49. Johnson JL, Rajagopalan KV. 1977. *J. Biol. Chem.* 252:2017–25
50. Southerland WM, Winge DR, Rajagopalan KV. 1978. *J. Biol. Chem.* 253:8747–52
51. Kubo Y, Ogura N, Nakagawa H. 1988. *J. Biol. Chem.* 263:19684–89
52. Neame PJ, Barber MJ. 1989. *J. Biol. Chem.* 264:20894–901
53. Crawford NM, Smith M, Bellissimo D, Davis RW. 1988. *Proc. Natl. Acad. Sci. USA* 85:5006–10
54. Cannons AC, Iida N, Solomonson LP. 1991. *Biochem. J.* 278:203–9
55. Hyde GE, Campbell WH. 1990. *Biochem. Biophys. Res. Commun.* 168:1285–91
56. Campbell WH. 1992. *Plant Physiol.* 99:693–99
57. Solomonson LP, Barber MJ. 1990. *Annu. Rev. Plant Physiol. Plant Mol. Biol.* 41:225–53
58. Lu GG, Campbell WH, Schneider G, Lindqvist Y. 1994. *Structure* 2:809–21
59. Lu GG, Lindqvist Y, Schneider G, Dwivedi U, Campbell WH. 1995. *J. Mol. Biol.* 248:931–48
60. George GN, Kipke CA, Prince RC, Sunde RA, Enemark JH, Cramer SP. 1989. *Biochemistry* 28:5075–80
61. Holm RH. 1987. *Chem. Rev.* 87:1401–49
62. Stiefel EI. 1973. *Proc. Natl. Acad. Sci. USA* 70:988–92
63. Garrett RM, Rajagopalan KV. 1996. *J. Biol. Chem.* 271:7387–91
64. Berg JM, Holm RH. 1984. *J. Am. Chem. Soc.* 106:3035–36
65. Berg JM, Holm RH. 1985. *J. Am. Chem. Soc.* 107:917–25
66. Roberts SA, Young CG, Kipke CA, Cleland WA, Yamanouchi K, et al. 1990. *Inorg. Chem.* 29:3650– 56
67. Gheller SF, Schultz BE, Scott MJ, Holm RH. 1992. *J. Am. Chem. Soc.* 114:6934–35
68. Xiao Z-G, Young CG, Enemark JH, Wedd AG. 1992. *J. Am. Chem. Soc.* 114:9194–95
69. Schultz BE, Holm RH. 1993. *Inorg. Chem.* 32:4244–48
70. Schultz BE, Gheller SF, Muetterties MC, Scott MJ, Holm RH. 1993. *J. Am. Chem. Soc.* 115:2714–22
71. Bray RC, Gutteridge S, Lamy MT, Wilkinson T. 1983. *Biochem. J.* 211:227–36
72. Pacheco A, Basu P, Borbat P, Raitsimring AM, Enemark JH. 1996. *Inorg. Chem.* 35:7001–8

72a. Trautwein T, Krauss F, Lottspeich F, Simon H. 1994. *Eur. J. Biochem.* 222: 1025–32

73. Oku H, Ueyama N, Nakamura A. 1996. *Chem. Lett.* 1996:31–32
74. Kraulis PJ. 1991. *J. Appl. Crystallogr.* 24:946–50

Annual Review of Biochemistry
Volume 66, 1997

CONTENTS